

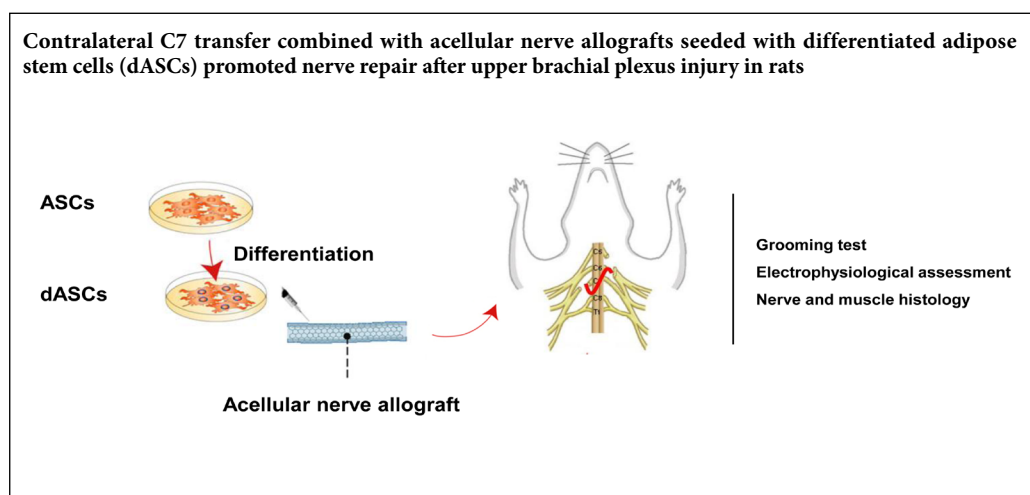
# Contralateral C7 transfer combined with acellular nerve allografts seeded with differentiated adipose stem cells for repairing upper brachial plexus injury in rats

Jian-Tao Yang<sup>‡</sup>, Jin-Tao Fang<sup>‡</sup>, Liang Li, Gang Chen, Ben-Gang Qin, Li-Qiang Gu<sup>\*</sup>

Department of Microsurgery & Orthopedic Trauma, the First Affiliated Hospital of Sun Yat-sen University, Guangzhou, Guangdong Province, China

**Funding:** This work was supported by the National Natural Science Foundation of China, No. 81601057 (to JTY).

## Graphical Abstract



**\*Correspondence to:**  
Li-Qiang Gu, MD, PhD,  
guliqiang1963@aliyun.com.

#These authors contributed equally to this study.

**orcid:**  
0000-0003-0532-5093  
(Li-Qiang Gu)

**doi:** 10.4103/1673-5374.259626

**Received:** December 29, 2018  
**Accepted:** May 21, 2019

## Abstract

Nerve grafting has always been necessary when the contralateral C7 nerve root is transferred to treat brachial plexus injury. Acellular nerve allograft is a promising alternative for the treatment of nerve defects, and results were improved by grafts laden with differentiated adipose stem cells. However, use of these tissue-engineered nerve grafts has not been reported for the treatment of brachial plexus injury. The aim of the present study was to evaluate the outcome of acellular nerve allografts seeded with differentiated adipose stem cells to improve nerve regeneration in a rat model in which the contralateral C7 nerve was transferred to repair an upper brachial plexus injury. Differentiated adipose stem cells were obtained from Sprague-Dawley rats and transdifferentiated into a Schwann cell-like phenotype. Acellular nerve allografts were prepared from 15-mm bilateral sections of rat sciatic nerves. Rats were randomly divided into three groups: acellular nerve allograft, acellular nerve allograft + differentiated adipose stem cells, and autograft. The upper brachial plexus injury model was established by traction applied away from the intervertebral foramen with micro-hemostat forceps. Acellular nerve allografts with or without seeded cells were used to bridge the gap between the contralateral C7 nerve root and C5–6 nerve. Histological staining, electrophysiology, and neurological function tests were used to evaluate the effect of nerve repair 16 weeks after surgery. Results showed that the onset of discernible functional recovery occurred earlier in the autograft group first, followed by the acellular nerve allograft + differentiated adipose stem cells group, and then the acellular nerve allograft group; moreover, there was a significant difference between autograft and acellular nerve allograft groups. Compared with the acellular nerve allograft group, compound muscle action potential, motor conduction velocity, positivity for neurofilament and S100, diameter of regenerating axons, myelin sheath thickness, and density of myelinated fibers were remarkably increased in autograft and acellular nerve allograft + differentiated adipose stem cells groups. These findings confirm that acellular nerve allografts seeded with differentiated adipose stem cells effectively promoted nerve repair after brachial plexus injuries, and the effect was better than that of acellular nerve repair alone. This study was approved by the Animal Ethics Committee of the First Affiliated Hospital of Sun Yat-sen University of China (approval No. 2016-150) in June 2016.

**Key Words:** nerve regeneration; peripheral nerve injury; brachial plexus injury; contralateral C7 nerve root; acellular nerve; adipose stem cells; Schwann cells; tissue engineering nerve; nerve grafting; nerve defect; neural regeneration

**Chinese Library Classification No.** R459.9; R364; R605

## Introduction

Traumatic brachial plexus injuries, a clinically severe peripheral nerve injury (Carlstedt et al., 2017), cause permanent disability of the body with significant socioeconomic implications (Krishnan et al., 2008). Although nerve transfers including accessory nerve (Songcharoen et al., 1996), phrenic nerve, and intercostal nerve are presently the primary methods to treat brachial plexus injuries, availability of donor nerves remains limited, especially for patients with accessory and phrenic nerve injuries (Krakauer et al., 1994; Flores et al., 2016). Contralateral C7 (CC7) nerve could be a reliable donor for repair of upper trunk injuries, as it could be transferred through a modified pre-spinal approach to improve the recovery of shoulder abduction and elbow flexion (Wang et al., 2012). However, the limited separable length of the CC7 nerve, as well as fibrosis and distal retraction of the injured nerve roots, obstruct direct suture to the recipient nerves (Xu et al., 2012). Therefore, nerve grafting is still needed to bridge the nerve gap.

Currently, nerve autograft is regarded as the “gold standard” to treat peripheral nerve defects, but unavoidable complications such as the sacrificing of a functional nerve, dysfunction of the donor site, and limited wide use of autologous nerve grafts (Fansa et al., 2003; Johnson et al., 2005; Battiston et al., 2017). With the rapid development of tissue engineering, an increasing number of animal studies (Gu et al., 2011; Pfister et al., 2011; Cerqueira et al., 2018; Patel et al., 2018) and clinical studies (Cho et al., 2012; He et al., 2015; Hu et al., 2016; Zhu et al., 2017) have confirmed that acellular nerve allografts (ANAs) can yield good results for repair of peripheral nerve defects; moreover they were considered to be ideal peripheral nerve grafts. However, reparative effects of ANAs decrease with increasing length of the nerve graft, potentially as a result of the loss of a normal environment created by living cells for the advancement of nerve regeneration (Walsh et al., 2009).

Schwann cells (SCs), which can promote nerve regeneration and are a source of trophic factors, remyelinate axons and restore nerve conduction (Bunge et al., 1994). Thus, SCs are the main cell type considered for the seeding of tissue-engineered nerve grafts (Hadlock et al., 2000; Evans et al., 2002). However, SCs cultured *in vitro* have poor proliferative ability and an insufficient number of cells may delay nerve repair. Moreover, ideal cells for transplantation should be easily obtained, proliferate rapidly, and not elicit an immunological reaction (Tohill et al., 2004). Therefore, adult stem cells are a promising alternative to SCs. Mesenchymal stem cells, which have the potential to extensively self-renew and differentiate into cells of different lineages (Pittenger et al., 1999), have been applied as alternatives to SCs for many years. Among them, adipose stem cells (ASCs) are easily obtained and isolated from adipose tissue, which is abundant, by conventional liposuction procedures; moreover, ASCs can be expanded in culture, thus representing ideal seed cells for nerve repair (Zuk et al., 2004; Jiang et al., 2008). Several studies showed that SCs differentiated from ASCs (dASCs), elicit good results for treating nerve defects when compos-

ed with ANAs (Wang et al., 2012; Ghoreishian et al., 2013). However, use of ANAs combined with dASCs for the treatment of brachial plexus injuries has rarely been reported, especially for CC7 nerve-based repair.

Therefore, the purpose of the present study was to evaluate the efficacy of CC7 nerve transfer combined with acellular nerve grafts seeded with SCs differentiated from ASCs to repair upper brachial plexus injuries in a rat model.

## Materials and Methods

### Animals

Thirty male specific-pathogen-free Sprague-Dawley rats weighing 200–300 g and aged 6 weeks, and 10 female rats weighing 100–120 g and aged 4 weeks were provided by the Experimental Animal Center of Sun Yat-sen University, China (Production License No. SCXK (Yue) 2016-0029). Ten female Sprague-Dawley rats were used for harvesting ASCs, while 12 Sprague-Dawley rats were used for harvesting of nerve allografts. Rats were housed under temperature- and light-controlled conditions (25°C, 55% humidity, 12:12 hour light/dark cycle), with free access to water and food.

Eighteen male adult SD rats were randomly divided into three groups: ANA, ANA + dASCs, and autograft with four bundles of sural nerve autografts. All experiments were approved by the Administration Committee of Experimental Animals of the First Affiliated Hospital of Sun Yat-sen University (Animal Experimental Ethical Inspection License No. 2016-150) in June 2016. The experimental procedure followed the United States National Institutes of Health Guide for the Care and Use of Laboratory Animals (NIH Publication No. 85-23, revised 1985).

### ASC isolation and culturing

As previously described, ASCs were harvested from the inguinal fat pad of 10 female SD rats (Xu et al., 2008). Briefly, debris and erythrocytes were removed from chopped adipose tissues by extensive washing with sterile phosphate-buffered saline (PBS). The washed fat tissue was dissociated for 1 hour at 37°C using 0.15% collagenase type I (Gibco, Carlsbad, CA, USA). Undissociated tissue was removed from the solution using a 100- $\mu$ m filter, and enzyme activity was neutralized using an equal volume of Dulbecco's Modified Eagle's Medium (DMEM) (Gibco) containing 10% fetal bovine serum (Gibco). After centrifugation at 1000  $\times$  g for 5 minutes, the cell pellet was resuspended in DMEM containing 10% fetal bovine serum. Cells were plated and incubated at 37°C, 5% CO<sub>2</sub>, and defined as passage 0.

### Differentiation of ASCs into SC phenotypes and immunostaining

The differentiation procedure employed was as previously described (Xu et al., 2008). Briefly, passage 3–5 cells were plated at a density of  $1 \times 10^5$  cells/cm<sup>2</sup> and cultured in DMEM/F12 (1:1) containing 20 ng/mL epidermal growth factor (Peprotech, Rocky Hill, NJ, USA), 20 ng/mL basic fibroblast growth factor (Peprotech), and B27 (1:50, Gibco). Medium was replaced every 3 days to achieve the formation of neurospheres.

For terminal differentiation, neurospheres were dissociated into single cells using trypsin, and then seeded onto poly-L-lysine-coated (Sigma, St Louis, MO, USA) six-well chamber slides at a density of  $2 \times 10^5$  cells/cm<sup>2</sup>. Differentiation medium was DMEM supplemented with 35 ng/mL all-trans retinoic acid (Sigma), 14  $\mu$ M forskolin (Sigma), 200 ng/mL heregulin-beta1 (Peprotech), and 10 ng/mL platelet-derived growth factor-BB (Peprotech).

After differentiation, cells were fixed for 10 minutes in 4% paraformaldehyde and washed three times with PBS. Subsequently, cells were permeabilized in 0.2% Triton-X/PBS and blocked for 1 hour with bovine serum albumin. The following primary antibodies were applied overnight at 4°C: S-100 (1:100; Santa Cruz Biotechnology, Santa Cruz, CA, USA), P75 (1:250; Santa Cruz Biotechnology) and glial fibrillary acidic protein (GFAP, 1:400; Santa Cruz Biotechnology). After 24 hours, slides were washed three times with PBS and incubated with secondary antibody at room temperature in the dark for 1 hour. Nuclei were labeled with 4',6-diamidino-2-phenylindole (DAPI, Sigma) and proteins were visualized using a goat anti-mouse IgG conjugated to Cy3 (Sigma).

#### Preparation of acellular nerve allografts

Rats were intraperitoneally anesthetized with pentobarbital sodium (50 mg/kg; Sigma). The sciatic nerve of each rat was harvested and cleaned, then immediately immersed in PBS. Chemical detergents were used for nerve segments to remove cellular components, as detailed elsewhere (Sondell et al., 1998; Wang et al., 2010). Briefly, the nerve was placed in deionized distilled water and agitated for 7 hours, and then washed in 3% Triton X-100 (Sigma) overnight, followed by incubation in 4% sodium deoxycholate for 24 hours. For sterilization, nerves were immersed in Cobalt-60 for 12 hours after washing in PBS. Finally, the nerve was stored in sterile PBS at 4°C until use.

#### Surgical procedures

Rats underwent identical surgical procedures: general anesthesia with pentobarbital (50 mg/kg, intraperitoneal) under aseptic conditions. The upper brachial plexus avulsion injury (Figure 1A and B) was established by steady moderate traction applied away from the intervertebral foramen with micro-hemostat forceps. The CC7 nerve root was excised (Figure 1C), pulled distally, and marked by 5-0 silk sutures. A chemically extracted 1.5-cm-long ANA with or without cells was used to bridge the 1.5-cm gap between the CC7 nerve root and C5–6 nerve (Figure 1D). For non-cell-laden acellular nerve grafts, the nerve gap between CC7 and C5–6 was bridged using only an ANA. For dASC-seeded acellular nerve grafts, 10  $\mu$ L of dASCs with a density of  $1 \times 10^7$ /mL were injected longitudinally into ANAs using a pipette without damaging the epineurium. In the autograft group, the 1.5-cm-long nerve defect was bridged by sural nerve autografts. All nerve grafts were sutured to the epineurium of the CC7 and C5–6 nerve stumps using 11-0 monofilament nylon sutures under 10 $\times$  magnification.

#### Functional evaluation

Functional recovery of the upper limb was examined using a modified grooming test (Bertelli et al., 1993), which was employed to assess external shoulder rotation, abduction, and elbow flexion. The function of each rat was evaluated once weekly commencing 2 weeks after surgery and until 16 weeks. Briefly, 1–3 mL of water was squirted over the animal's snout to induce a reproducible grooming movement. Uninjured rats elevated both forelimbs to behind the ear, brought them down to the snout, and finally licked. This motion was recorded to evaluate the function of the bilateral forelimb. The onset of discernible function of the rat upper limb was recorded. Scores for the grooming test (Terzis grades) were defined as follows: 5 points, the paw touched behind the ear; 4 points, the paw reached the front of the ear, but not the back; 3 points, the paw reached the snout, but not the eye; 2 points, the paw touched the snout with flexion of the elbow; and 1 point, the paw could not touch the snout.

#### Electrophysiological assessment

Sixteen weeks after surgery, rats were anesthetized and the nerve grafting was exposed. Stimulating crook-shaped silver needle electrodes were placed on the proximal and distal sides of the nerve graft. Compound muscle action potentials of biceps or deltoid muscles were recorded using a biological function experimental system (BL-420F; TaiMeng, Inc., Chengdu, China). Motor conduction velocity was calculated using the latencies and distance from the stimulating to recording electrodes.

#### Histology of the regenerated nerve

After electrophysiological evaluations, rats were sacrificed to excise the nerve segments ( $n = 6$ ). The distal stump of the regenerated nerve was harvested and fixed in 4% paraformaldehyde at 4°C overnight for immunohistochemical analysis. Hematoxylin-eosin staining of sections was used to analyze the basic structure of the regenerated nerve. In addition, nerve sections were incubated in a solution of monoclonal S-100 protein antibody (1:200; Sigma) and neurofilament (NF) antibody (1:200; Sigma) at room temperature for 2 hours. Subsequently, nerve sections were incubated in anti-rabbit IgG solution (1:300; Jackson ImmunoResearch, West Grove, PA, USA) for 30 minutes. Six randomly selected areas of each nerve section were captured to quantify S-100- and NF-positive areas using Image Pro Plus 6.0 software (Media Cybernetics, Silver Spring, MD, USA).

#### Evaluation of regenerated nerve myelination

For the middle part of regenerated nerves, a 1- to 2-mm slice cut at the proximal part was placed in 2.5% glutaraldehyde for 2 hours, osmicated, dehydrated, and embedded in Epon 812 resin (Ted Pella, Redding, PA, USA). A transverse section (1  $\mu$ m) was stained with 1% toluidine blue. Axon density based on the total number of myelinated axons was calculated. Six random pictures of each sample were captured to quantify the number of axons. Thickness of the myelin sheath, diameter of the myelinated axon, and ratio of the

axon to the total fiber diameter were quantified from transmission electron microscope images. In total, 50–60 random axons from each specimen were assessed.

### Morphology of the muscle

Before excising nerve segments, deltoid and biceps muscles on the experimental side were harvested. Acetylcholinesterase (AChE) cytochemical staining was used to observe the motor endplates. The remaining muscle samples were fixed with 4% formalin, embedded in paraffin, and transversely sectioned with a cryostat. Sections were stained with Masson trichrome and observed by light microscopy. Four randomly selected fields of each specimen were analyzed to measure the muscle fibers area. The percentage of collagen fibers is expressed as the area of collagen divided by the total area of muscle and collagen.

### Statistical analysis

All data are expressed as the mean  $\pm$  SD, and were analyzed using SPSS 15.0 software (SPSS, Chicago, IL, USA). One-way analysis of variance was employed to assess significant differences among the three groups.  $P < 0.05$  was considered statistically significant.

## Results

### Characterization and immunocytochemical analysis of SCs

ASCs displayed a population of spindle-shaped cells (Figure 2A). ASCs were then re-cultured in DMEM/F12 medium supplemented with basic fibroblast growth factor, epidermal growth factor, and B27. After 2–4 days, many neurospheres were observed (Figure 2B and C). The neurospheres were triturated into single cells, which were then re-cultured in differentiation medium. After culture for an additional 2–4 days, cells were elongated, growing in a longitudinal and SC-like shape (Figure 2D–F). To evaluate the differentiation of SC-like cells, immunocytochemical analysis of SC markers (GFAP, P75, and S100) was assessed after 9 days. The results indicated that expression of GFAP, P75, and S100 in SC-like cells was noticeably increased in all groups (Figure 3A, B and C).

### Motor function assessment

Before surgery, rats could raise their forelimbs and reach the area behind their ears. However, rats receiving CC7 nerve repair displayed great improvement when testing these movements, especially in the autograft group. The onset of discernible function of the autograft group ( $45.40 \pm 7.30$  days) was later than observed in ANA + dASCs and ANA groups ( $53.20 \pm 3.35$  days, and  $61.40 \pm 6.80$  days, respectively) (Figure 4A). However, no statistical significance was found between autograft and ANA + dASCs groups ( $P > 0.05$ ). Sixteen weeks after nerve grafting, all three groups showed clear signs of functional recovery of the forelimb. Terzis grades of the autograft group ( $3.60 \pm 0.55$ ) were higher than in ANA and ANA + dASCs groups ( $3.20 \pm 0.45$  and  $3.40 \pm 0.55$ , respectively), although there was no statistical significance

among the three groups (Figure 4B).

An electrophysiological assessment was performed to investigate whether functional reinnervation occurred. The percentage of compound muscle action potential amplitude calculated on injured and contralateral sides for each group was significantly increased in the autograft group compared with ANA and ANA + dASCs groups ( $P < 0.05$ ). The percentage of compound muscle action potential amplitude was significantly increased in the ANA + dASCs group compared with the ANA group ( $P < 0.05$ ; Figure 4C). Motor conduction velocity value was highest in the autograft group among all three groups. Motor conduction velocity was increased in the ANA + dASCs group compared with the ANA group ( $P < 0.05$ ; Figure 4D).

### Histological assessment of regenerated nerves

Sixteen weeks postoperatively, linearly ordered structures were observed in the newly formed nerves for all three groups using hematoxylin-eosin staining (Figure 5A). NF200 and S100 staining was performed on nerve specimens of each group to quantify nerve axons and SC survival, respectively. Positive expression of NF-200 and S100 was both observed in regenerated nerves of the three groups (Figure 5B and C). Percentages of S100-positive and NF-positive areas in autograft and ANA + dASCs groups were significantly increased compared with the ANA group at 16 weeks after surgery ( $P < 0.05$ ; Figure 5D and E). However, there was no significant difference between autograft and ANA + dASCs groups ( $P > 0.05$ ).

### Remyelination of nerves

Sixteen weeks postoperatively, toluidine blue staining (Figure 6A) and transmission electron microscopic examination (Figure 6B) were used to compare nerve remyelination of the middle implants of each group. Few myelinated fibers were observed in the ANA group, which presented more debris. Compared with the ANA group, nerve fibers and abundant myelinated fibers were regularly arranged in autograft and ANA + dASCs groups. Moreover, the number and diameter of myelinated axons were greatest in the autograft group, followed by ANA + dASCs and ANA groups ( $P < 0.01$ ; Figure 6C and D). Thickness of the myelin sheath was significantly increased in autograft and ANA + dASCs groups compared with the ANA group ( $P < 0.05$ ; Figure 6E). However, there was no significant difference in G-ratio among the groups (Figure 6F).

### Examination of muscles

Masson trichrome staining of the target muscle morphology was performed at 16 weeks post-operation (Figure 7A). AChE staining was used to evaluate the motor end plate units of target muscles (Figure 7B), further indicating the reduction of muscle atrophy in autograft and ANA + dASCs groups because of enhanced muscle reinnervation after nerve repair. However, motor endplates were rarely present in the ANA group. Masson staining results indicated that the cross-sectional area of the muscle fiber was significantly

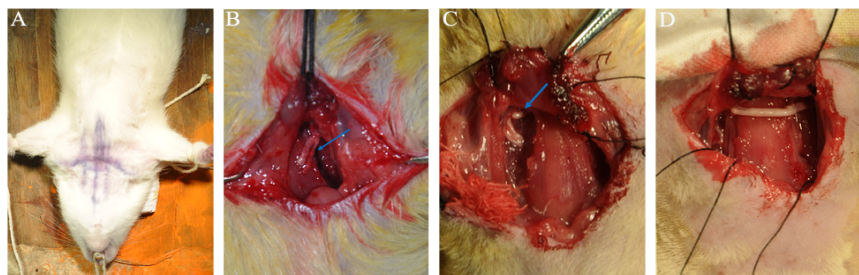


**Figure 1 Surgical procedures.**  
 (A) A midline incision was performed. (B) The C5–6 distal stumps of the injured side are indicated by blue arrows. (C) The contralateral C7 was fully exposed and is also indicated by blue arrows. (D) The nerve defect between contralateral C7 and C5–6 distal stumps were bridged by nerve graft.

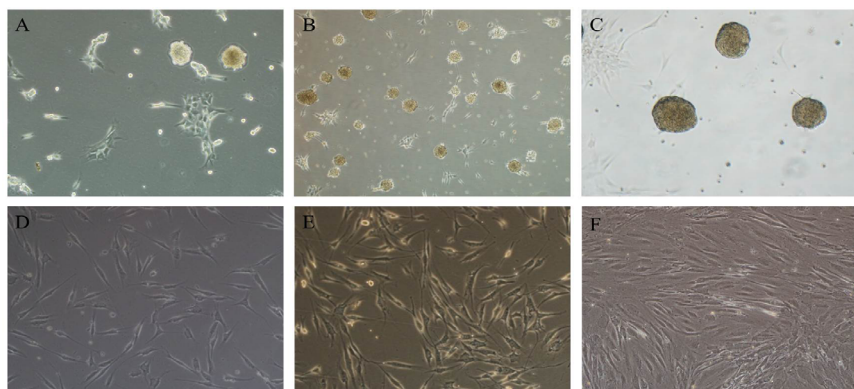


**Figure 2 Morphological changes in adult adipose-derived stromal cells before and after induction (inverted contrast microscopy).**  
 (A) After re-culture in Dulbecco's Modified Eagle's Medium/F12 containing epidermal growth factor, basic fibroblast growth factor, and B27 for 24 hours, a heterogeneous population of spindle-shaped cells was observed. (B, C) After continuing culture for 2–4 days, neurospheres were observed. (D, E) After culture for an additional 2–4 days, cells were elongated and growing in a longitudinal and Schwann cell-like shape. (F) Morphology of adult adipose-derived stromal cells in the control group showed no change. Original magnification, 100×.

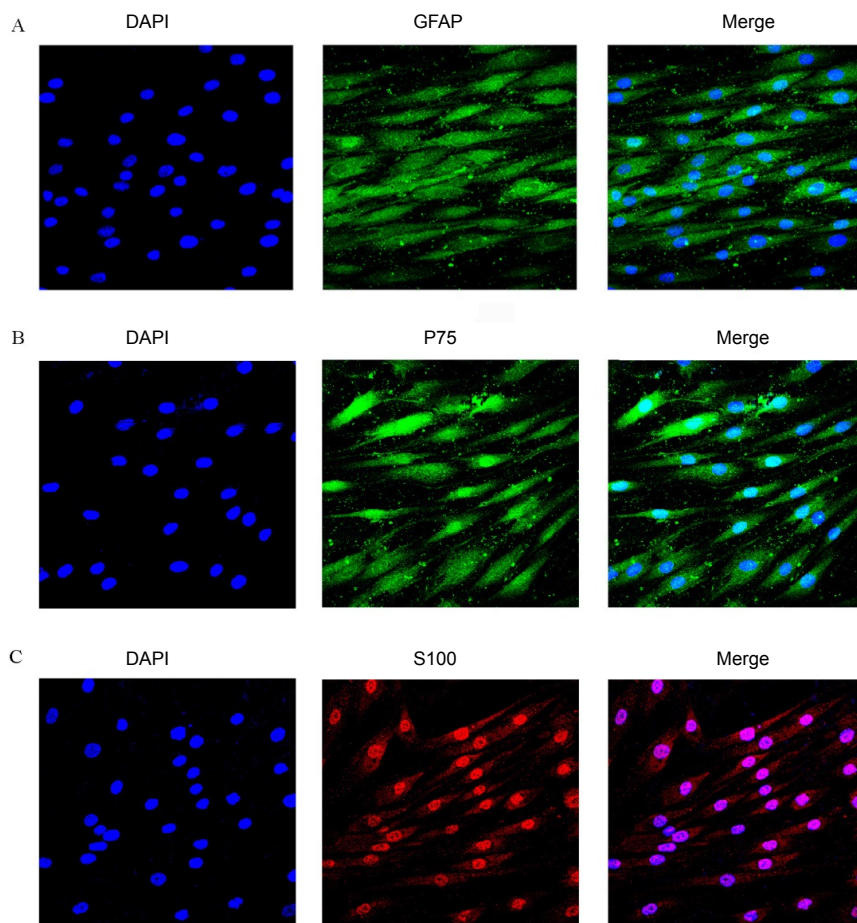


**Figure 3 Immunostaining of differentiated adipose stem cells after 9 days (fluorescence microscope).**  
 (A–C) Nearly all Schwann cell-like cells expressed specific markers: (A) GFAP, (B) P75, and (C) S-100. All nuclei were counterstained with DAPI (blue). GFAP: Glial fibrillary acidic protein; DAPI: 4',6-diamidino-2-phenylindole. Original magnification, 400×.

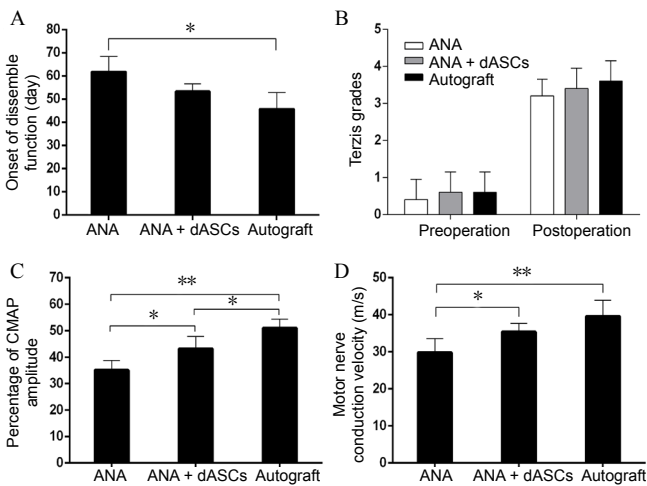


**Figure 4** Histograms showing functional recovery of the upper limb in the three groups. (A) Onset of discernible function of each group. (B) Terzis grades (grooming test) in each group before and after surgery, indicating functional improvement of the forelimb in all groups 16 weeks after surgery. (C, D) CMAP recovery ratio and motor conduction velocity on the intervention side at 16 weeks after nerve grafting. \* $P < 0.05$ , \*\* $P < 0.01$  (mean  $\pm$  SD,  $n = 6$ ; one-way analysis of variance followed by least significant difference *post hoc* test). CMAP: Compound muscle action potential; ANA: acellular nerve allografts; dASCs: differentiated adipose stem cells.

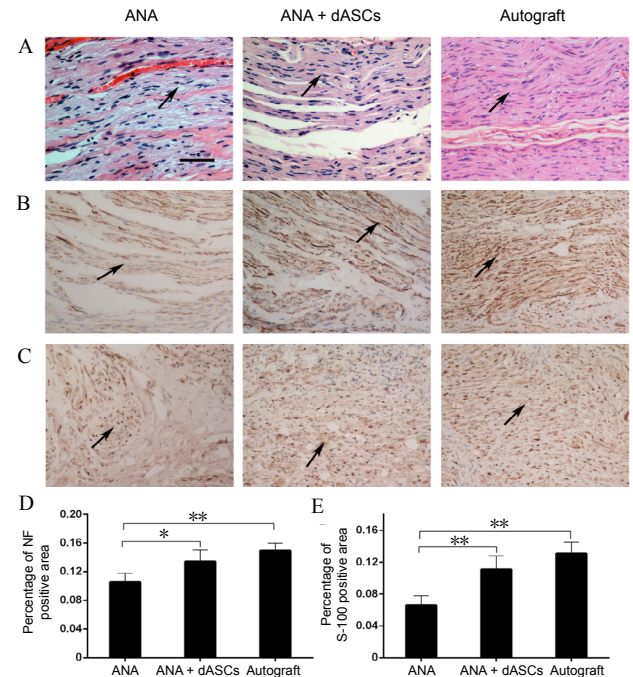
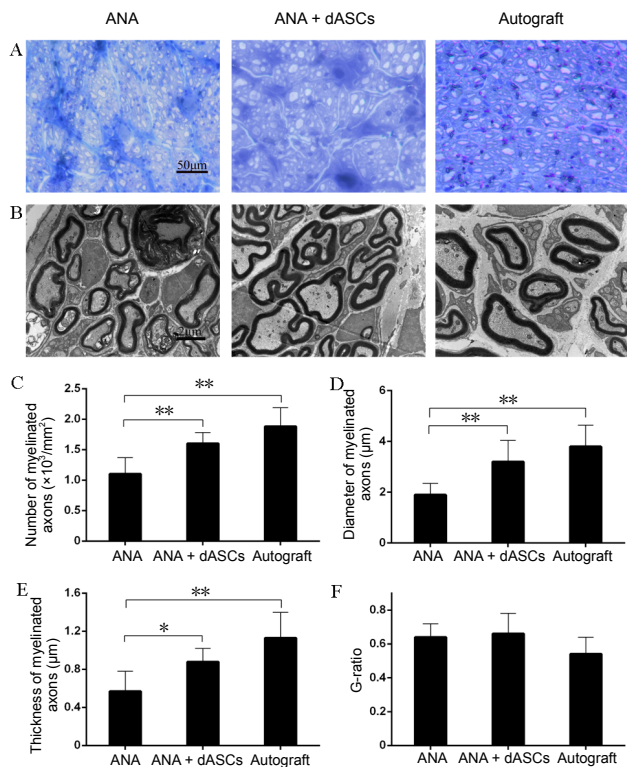


**Figure 5** Histological analysis of the regenerated nerve at 16 weeks after nerve grafting. (A) Hematoxylin-eosin staining of nerve grafts: the arrows indicates that autograft and ANA + dASCs groups provided more newly formed nerves than the ANA group. (B) Immunostaining for NF. (C) Immunostaining for S-100, the arrows indicates that both autograft and ANA + dASCs groups exhibited increased percentages of S-100- and NF-positive areas compared with the ANA group. Inverted contrast microscopy, original magnification, 100 $\times$ . Scale bar: 50  $\mu\text{m}$ . (D, E) Significant increases in numbers of positively stained S-100 and NF in autograft and ANA + dASCs groups compared with the ANA group. \* $P < 0.05$ , \*\* $P < 0.01$  (mean  $\pm$  SD,  $n = 6$ ; one-way analysis of variance followed by least significant difference *post hoc* test). NF: Neurofilament; ANA: acellular nerve allografts; dASCs: differentiated adipose stem cells.

**Figure 6** Remyelination of the regenerated nerve. (A) Toluidine blue staining results: The number of regenerating nerve fibers was increased in autograft and ANA + dASCs groups compared with the ANA group. Original magnification, 400 $\times$ . Scale bar: 50  $\mu\text{m}$ . (B) Transmission electron microscopy results: Axon bundling and myelination were reduced in the ANA group compared with autograft and ANA + dASCs groups. Transmission electron microscopy, Scale bar: 2  $\mu\text{m}$ , original magnification, 15000 $\times$ . The number (C), diameter (D), and thickness of myelinated axons (E) were significantly increased in autograft and ANA + dASCs groups compared with the ANA group. (F) G-ratio among the three groups. \* $P < 0.05$ , \*\* $P < 0.01$  (mean  $\pm$  SD,  $n = 6$ ; one-way analysis of variance followed by least significant difference *post hoc* test). ANA: Acellular nerve allografts; dASCs: differentiated adipose stem cells.

**Figure 7** Examination of the muscles. (A, B) Masson trichrome staining and cholinesterase staining of the motor endplate of the biceps: muscle atrophy was reduced and more motor endplates were present in autograft and ANA + dASCs groups. Inverted contrast microscopy, original magnification, 100 $\times$ . Scale bar: 200  $\mu\text{m}$ . (C, D) Cross-sectional area of muscle fibers and percentage of collagen fiber area for biceps on the surgical sides. \* $P < 0.05$ , \*\* $P < 0.01$  (mean  $\pm$  SD,  $n = 6$ ; one-way analysis of variance followed by least significant difference *post hoc* test). ANA: Acellular nerve allografts; dASCs: differentiated adipose stem cells.

increased in autograft and ANA + dASCs groups compared with the ANA group ( $P < 0.05$ ; **Figure 7C**). Moreover, among the three groups, average percentage of collagen fiber area of the target muscle on the injured side was largest in the ANA group ( $P < 0.05$ ; **Figure 7D**).

## Discussion

The CC7 nerve root is a reliable donor for the treatment of brachial plexus injury, as it can be transferred through a pre-spinal approach to the avulsed upper trunk to improve the recovery of shoulder abduction and elbow flexion (Xu et al., 2008; Wang et al., 2012). In addition, nerve autografts, such as sural nerve, are commonly required to bridge the gap between CC7 and the upper trunk or C5–6 nerve roots, as direct repair cannot be achieved for all patients without unavoidable complications at the donor site. Human ANAs, also known as processed nerve allografts, have been successfully used for repair of nerve defects in clinical practice (Rinker et al., 2017). However, the application of ANAs combined with dASCs in brachial plexus root avulsion injury has rarely been reported, especially for CC7 nerve root transfer.

As variables that influence nerve regeneration can be better controlled in animal experiments compared with clinical research (Navarro et al., 2009), we devised a repair model in which the CC7 nerve root was transferred to the upper trunk through a modified anterior spinal approach to evaluate the effect of ANAs on nerve regeneration. However, we found that the outcome of a pre-spinal route for CC7 transfer was not ideal and rat mortality was very high, although efforts were made in early experiments. There are several reasons accounting for this result. First, the blood supply of the anterior spinal zone was easily damaged when making the anterior spinal route, thus increasing the morbidity of intraoperative and postoperative bleeding. Second, the narrow space of the anterior spinal route easily resulted in nerve compression and the length of the dissected C7 nerve root was not long enough to place through this route, causing great difficulties in nerve anastomosis. Third, unlike patients in clinical practice, recovery of rats from anesthesia was rapid and the motion of the trachea and esophagus pressed against the vertebrae when rats started to eat or drink, which would also cause nerve compression, thus affecting nerve regeneration. Therefore, we modified the animal model using a subcutaneous tunnel through the superficial muscles of the neck to avoid the aforementioned disadvantages.

ANAs have been shown to improve nerve regeneration without immune responses or infection (Moore et al., 2009; Tajdaran et al., 2016). However, unlike nerve autografts, acellular grafts lack a beneficial microenvironment for axonal regeneration and are unable to provide full functional recovery (Wang et al., 2015). Therefore, an appropriate microenvironment is necessary for nerve regeneration and target reinnervation. In our previous animal studies, better functional outcomes were achieved when the ANA was used in combination with platelet-rich plasma, Etifoxine, or ginkgo biloba extract (Zhu et al., 2015). Zheng et al. (2014) demonstrated that platelet-rich plasma stimulated SC prolifer-

ation and migration, increased expression of nerve growth factor (NGF) and glial-derived neurotrophic factor (GDNF), and improved axon regeneration. Zhou et al. (2014) also discovered that etifoxine enhanced synthesis of neurotrophic factors, including NGF, GDNF, and vascular endothelial growth factor, and promoted nerve regeneration.

In addition, some studies have shown that SCs improved nerve regeneration when seeded with tubular nerve conduits (Kingham et al., 2007; Kalbermatten et al., 2008; Jiang et al., 2017). However, disadvantages such as immune rejection continue to hinder wide application of SCs for allografting. ASCs have been identified as suitable alternatives to SCs for tissue-engineering nerves, as they are easily accessible and can be differentiated into SCs (Schaakxs et al., 2008; Georgiou et al., 2015). Several research groups have shown that ANA seeded with ASCs, bone marrow mesenchymal stem cells, or SC-like cells achieved better functional recovery in repairing peripheral nerve defects (Liu et al., 2011; Fan et al., 2014; Jesuraj et al., 2014; Wang et al., 2016). Our study also demonstrated that ASCs, which were isolated from adipose tissue and exposed to differentiation media, produced a morphological change into an elongated spindle phenotype and expression of specific glial markers, including GFAP, p75 and S100, suggesting plenty of SCs were produced from ASCs. In the present study, nerve root avulsion rats transferred with CC7 combined with ANAs laden with dASCs exhibited significantly better function compared with the ANA group. Moreover, the ANA + dASCs group showed increased axon regeneration and myelination, and reduced muscle atrophy, similar to the nerve autograft group.

The present study assessed nerve regeneration in ANA, ANA + dASCs, and autograft groups at 16 weeks after nerve grafting. First, a grooming test was used to evaluate the recovery of motor function in the post-operative affected forelimb, as described by Bertelli and Mira (1993). After surgery, normal grooming actions were not observed in any of the three groups, indicating dysfunction of the shoulder and elbow. It has been reported that muscle atrophy is irreversible after nerve injury and the functional outcome would be poor if axons did not regenerate into distal target muscles (Zheng et al., 2014). Therefore, rapid regeneration of nerves is of great importance in peripheral nerve regeneration. Our results showed earlier functional recovery of grooming in the ANA + dASCs group compared with the ANA group, demonstrating that ANA seeded with SCs could accelerate nerve regeneration; although, the results were not as satisfactory as the autograft group. Gao et al. (2014) also reported the use of ANAs seeded with dASCs for 10-mm sciatic nerve defects in Sprague-Dawley rats, which resulted in remarkably improved results over ANAs but were similar to autograft at 6 and 12 weeks after surgery, similar to our results. However, in the present study, shoulder abduction and elbow flexion of the three groups were all recovered at 16 weeks post-surgery, and there was no significant difference in scores among the three groups. This may be associated with the long-term process of central cortex remodeling after CC7 nerve root transfer.

Histological evaluation of regenerated nerve and muscle 16 weeks after surgery was used to assess nerve regeneration. Immunohistochemistry provided clear evidence that percentages of NF and S-100 positively stained areas in the ANA + dASCs group were increased compared with the ANA group, and were almost identical to the autograft group. Additionally, myelinated fiber density was highest in the autograft group, followed by ANA + dASCs and ANA groups. The results of histological evaluation of the target muscle showed that compared with the ANA group, more regenerated axons grew through the ANA + dASCs to reinnervate the target. These findings may indicate that dASCs, which have the ability to produce neurotrophic and neurotropic factors, could support and maintain the regeneration of peripheral nervous system axons, thus enhancing neural recovery. Extracellular matrix, the main component of ANA, is very important for cell survival, differentiation, and migration. A study by di Summa et al. (2014) demonstrated that extracellular matrix molecules noticeably improved the potential of dASCs for axon regeneration. However, further study is needed to better understand this finding.

As far as we know, this may be the first report of ANAs incorporating SCs, which were differentiated from ASCs, for use as nerve grafts to bridge the defect nerve gap when CC7 nerve root transfer was performed in a rat upper brachial plexus root avulsion model. The efficacy for stimulating myelinated axon regeneration and rescuing muscle atrophy in the ANA + dASCs group was better than that observed in the ANA group, and almost identical to the autograft group.

In summary, the model of CC7 nerve transfer combined with nerve grafts seeded with dASCs through superficial muscles of the neck was reliable for nerve repair after brachial plexus injury. Moreover, as confirmed by functional measures, histology, and electrophysiological examination, this method effectively promoted axon regeneration and muscle reinnervation, and effectively restored shoulder and elbow functions after upper brachial plexus injuries; thus, providing an experimental basis for future clinical use.

**Author contributions:** Study design: BGQ, LQG; experimental implementation, data analysis: JTY, JTF; data and picture collection: LL and GC; paper writing: JTY. All authors approved the final version of the paper.  
**Conflicts of interest:** All authors must disclose any financial and personal relationships with other people or organizations that could inappropriately influence (bias) their work.

**Financial support:** This work was supported by the National Natural Science Foundation of China, No. 81601057 (to JTY). The funding source had no role in study conception and design, data analysis or interpretation, paper writing or deciding to submit this paper for publication.

**Institutional review board statement:** All animal experimental procedures were approved by the Ethics Committee of the First Affiliated Hospital of Sun Yat-sen University of China (approval No. 2016-150) in June 2016.

**Copyright license agreement:** The Copyright License Agreement has been signed by all authors before publication.

**Data sharing statement:** Datasets analyzed during the current study are available from the corresponding author on reasonable request.

**Plagiarism check:** Checked twice by iThenticate.

**Peer review:** Externally peer reviewed.

**Open access statement:** This is an open access journal, and articles are distributed under the terms of the Creative Commons Attribution-Non-Commercial-ShareAlike 4.0 License, which allows others to

remix, tweak, and build upon the work non-commercially, as long as appropriate credit is given and the new creations are licensed under the identical terms.

**Open peer reviewer:** Ioannis Gkiatas, University of Ioannina, School of Medicine, Greece.

**Additional file:** Open peer review report 1.

## References

- Battiston B, Titolo P, Ciclamini D, Panero B (2017) Peripheral nerve defects: overviews of practice in Europe. *Hand Clin* 33:545-550.
- Bertelli JA, Mira JC (1993) Behavioral evaluating methods in the objective clinical assessment of motor function after experimental brachial plexus reconstruction in the rat. *J Neurosci Methods* 46:203-208.
- Boriani F, Fazio N, Bolognesi F, Pedrini FA, Marchetti C, Baldini N (2019) Noncellular modification of acellular nerve allografts for peripheral nerve reconstruction: a systematic critical review of the animal literature. *World Neurosurg* 122:692-703.
- Bunge RP (1994) The role of the Schwann cell in trophic support and regeneration. *J Neurol* 242: S19-21.
- Carlstedt T, James N, Risling M (2017) Surgical reconstruction of spinal cord circuit provides functional return in humans. *Neural Regen Res* 12:1960-1963.
- Cerqueira SR, Lee YS, Cornelison RC, Mertz MW, Wachs RA, Schmidt CE, Bunge MB (2018) Decellularized peripheral nerve supports Schwann cell transplants and axon growth following spinal cord injury. *Biomaterials* 177:176-185.
- Cho MS, Rinker BD, Weber RV, Chao JD, Ingari JV, Brooks D, Buncke GM (2012) Functional outcome following nerve repair in the upper extremity using processed nerve allograft. *J Hand Surg Am* 37:2340-2349.
- di Summa PG, Kalbermatten DE, Raffoul W (2013) Extracellular matrix molecules enhance the neurotrophic effect of Schwann cell-like differentiated adipose-derived stem cells and increase cell survival under stress conditions. *Tissue Eng Part A* 19:368-379.
- Evans GR, Brandt K, Katz S (2002) Bioactive poly (L-lactic acid) conduits seeded with Schwann cells for peripheral nerve regeneration. *Biomaterials* 23:841-848.
- Fan L, Yu Z, Li J, Dang X, Wang K (2014) Schwann-like cells seeded in acellular nerve grafts improve nerve regeneration. *BMC Musculoskelet Disord* 15:165.
- Fansa H, Dodic T, Wolf G, Schneider W, Keilhoff G (2003) Tissue engineering of peripheral nerves: epineurial grafts with application of cultured Schwann cells. *Microsurgery* 23:72-77.
- Flores LP, Socolovsky M (2016) Phrenic nerve transfer for reconstruction of elbow extension in severe brachial plexus injuries. *J Reconstr Microsurg* 32:546-550.
- Gao S, Zheng Y, Cai Q (2014) Combination of acellular nerve graft and Schwann cells-like cells for rat sciatic nerve regeneration. *Neural Plast* 14:139085.
- Georgiou M, Golding JP, Loughlin AJ, Kingham PJ, Phillips JB (2015) Engineered neural tissue with aligned, differentiated adipose-derived stem cells promotes peripheral nerve regeneration across a critical sized defect in rat sciatic nerve. *Biomaterials* 37:242-251.
- Ghoreishian M, Rezaei M, Beni BH (2013) Facial nerve repair with Gore-Tex tube and adipose-derived stem cells: an animal study in dogs. *J Oral Maxillofac Surg* 71:577-587.
- Gu X, Ding F, Yang Y, Liu J (2011) Construction of tissue engineered nerve grafts and their application in peripheral nerve regeneration. *Prog Neurobiol* 93:204-230.
- Hadlock T, Sundback C, Hunter D, Cheney M, Vacanti JP (2000) A polymer foam conduit seeded with Schwann cells promotes guided peripheral nerve regeneration. *Tissue Eng* 6:119-127.
- He B, Zhu Q, Chai Y (2015) Safety and efficacy evaluation of a human acellular nerve graft as a digital nerve scaffold: a prospective, multi-centre controlled clinical trial. *J Tissue Eng Regen Med* 9:286-295.

- Hu M, Xiao H, Niu Y, Liu H, Zhang L (2016) Long-term follow-up of the repair of the multiple-branch facial nerve defect using acellular nerve allograft. *J Oral Maxillofac Surg* 74:218.
- Jesuraj NJ, Santosa KB, Macewan MR, Moore AM, Kasukurthi R, Ray WZ, Flagg ER, Hunter DA, Borschel GH, Johnson PJ, Mackinnon SE, Sakiyama-Elbert SE (2014) Schwann cells seeded in acellular nerve grafts improve functional recovery. *Muscle Nerve* 49:267-276.
- Jiang L, Jones S, Jia X (2017) Stem cell transplantation for peripheral nerve regeneration: current options and opportunities. *Int J Mol Sci* 18:E94.
- Jiang L, Zhu JK, Liu XL (2008) Differentiation of rat adipose tissue-derived stem cells into Schwann-like cells in vitro. *Neuroreport* 19:1015-1019.
- Johnson EO, Zoubos AB, Soucacos PN (2005) Regeneration and repair of peripheral nerves. *Injury* 36 Suppl 4:S24-29.
- Kalbermatten DF, Kingham PJ, Mahay D (2008) Fibrin matrix for suspension of regenerative cells in an artificial nerve conduit. *J Plast Reconstr Aesthet Surg* 61:669-675.
- Kingham PJ, Kalbermatten DF, Mahay D, Armstrong SJ, Wiberg M, Terenghi G (2007) Adipose-derived stem cells differentiate into a Schwann cell phenotype and promote neurite outgrowth in vitro. *Exp Neurol* 207:267-274.
- Krakauer JD, Wood MB (1994) Intercostal nerve transfer for brachial plexopathy. *J Hand Surg Am* 19:829-835.
- Krishnan KG, Martin KD, Schackert G (2008) Traumatic lesions of the brachial plexus: an analysis of outcomes in primary brachial plexus reconstruction and secondary functional arm reanimation. *Neurosurgery* 62:873-885.
- Liu G, Cheng Y, Guo S (2011) Transplantation of adipose-derived stem cells for peripheral nerve repair. *Int J Mol Med* 28:565-572.
- Moore AM, MacEwan M, Santosa KB (2011) Acellular nerve allografts in peripheral nerve regeneration: a comparative study. *Muscle Nerve* 44:221-234.
- Navarro X, Udina E (2009) Methods and protocols in peripheral nerve regeneration experimental research: part III-electrophysiological evaluation. *Int Rev Neurobiol* 87:105-126.
- Patel NP, Lyon KA, Huang JH (2018) An update-tissue engineered nerve grafts for the repair of peripheral nerve injuries. *Neural Regen Res* 13:764-774.
- Pfister BJ, Gordon T, Loverde JR (2011) Biomedical engineering strategies for peripheral nerve repair: surgical applications, state of the art, and future challenges. *Crit Rev Biomed Eng* 39:81-124.
- Pittenger MF, Mackay AM, Beck SC (1999) Multilineage potential of adult human mesenchymal stem cells. *Science* 284:143-147.
- Rinker B, Zoldos J, Weber RV, Ko J, Thayer W, Greenberg J, Leversedge FJ, Safa B, Buncke G (2017) Use of processed nerve allografts to repair nerve injuries greater than 25 mm in the hand. *Ann Plast Surg* 78:S292-295.
- Schaakxs D, Kalbermatten DF, Pralong E (2017) Poly-3-hydroxybutyrate strips seeded with regenerative cells are effective promoters of peripheral nerve repair. *J Tissue Eng Regen Med* 11:812-821.
- Sondell M, Lundborg G, Kanje M (1998) Regeneration of the rat sciatic nerve into allografts made acellular through chemical extraction. *Brain Res* 795:44-54.
- Songcharoen P, Mahaisavariya B, Chotigavanich C (1996) Spinal accessory neurotization for restoration of elbow flexion in avulsion injuries of the brachial plexus. *J Hand Surg Am* 21:387-390.
- Tajdaran K, Gordon T, Wood MD, Shoichet MS, Borschel GH (2016) A glial cell line-derived neurotrophic factor delivery system enhances nerve regeneration across acellular nerve allografts. *Acta Biomater* 29:62-70.
- Tohill MP, Mann DJ, Mantovani CM, Wiberg M, Terenghi G (2004) Green fluorescent protein is a stable morphological marker for Schwann cell transplants in bioengineered nerve conduits. *Tissue Eng* 10:1359-1367.
- Walsh S, Biernaskie J, Kemp SW, Midha R (2009) Supplementation of acellular nerve grafts with skin derived precursor cells promotes peripheral nerve regeneration. *Neuroscience* 164:1097-107.
- Wang D, Liu XL, Zhu JK (2010) Repairing large radial nerve defects by acellular nerve allografts seeded with autologous bone marrow stromal cells in a monkey model. *J Neurotrauma* 27:1935-1943.
- Wang EW, Zhang J, Huang JH (2015) Repairing peripheral nerve injury using tissue engineering techniques. *Neural Regen Res* 10:1393-1394.
- Wang S, Yiu HW, Li P (2012) Contralateral C7 nerve root transfer to neurotize the upper trunk via a modified prespinal route in repair of brachial plexus avulsion injury. *Microsurgery* 32:183-188.
- Wang Y, Jia H, Li WY, Guan LX, Deng L, Liu YC, Liu GB (2016) Molecular examination of bone marrow stromal cells and chondroitinase ABC-assisted acellular nerve allograft for peripheral nerve regeneration. *Exp Ther Med* 12:1980-1992.
- Wang Y, Zhao Z, Ren Z (2012) Recellularized nerve allografts with differentiated mesenchymal stem cells promote peripheral nerve regeneration. *Neurosci Lett* 514:96-101.
- Xu L, Gu Y, Xu J (2008) Contralateral C7 transfer via the prespinal and retropharyngeal route to repair brachial plexus root avulsion: a preliminary report. *Neurosurgery* 63:553-558.
- Xu Y, Liu Z, Liu L (2008) Neurospheres from rat adipose-derived stem cells could be induced into functional Schwann cell-like cells in vitro. *Bmc Neurosci* 9:21.
- Zheng C, Zhu Q, Liu X (2014) Improved peripheral nerve regeneration using acellular nerve allografts loaded with platelet-rich plasma. *Tissue Eng Part A* 20:3228-3240.
- Zhou X, He B, Zhu Z (2014) Etifoxine provides benefits in nerve repair with acellular nerve grafts. *Muscle Nerve* 50:235-243.
- Zhu S, Liu J, Zheng C (2017) Analysis of human acellular nerve allograft reconstruction of 64 injured nerves in the hand and upper extremity: a 3 year follow-up study. *J Tissue Eng Regen Med* 11:2314-2322.
- Zhu Z, Zhou X, He B (2015) Ginkgo biloba extract (EGb 761) promotes peripheral nerve regeneration and neovascularization after acellular nerve allografts in a rat model. *Cell Mol Neurobiol* 35:273-282.
- Zuk PA, Zhu M, Ashjian P (2002) Human adipose tissue is a source of multipotent stem cells. *Mol Biol Cell* 13:4279-4295.

P-Reviewer: Gkiatas I; C-Editor: Zhao M; S-Editors: Wang J, Li CH; L-Editors: Deussen AV, Pack M, Qiu Y, Song LP; T-Editor: Jia Y